

Implementation of the H- ϕ formulation in COMSOL Multiphysics for simulating the magnetization of bulk superconductors and comparison with the H-formulation

Alexandre Arsenault¹, Frédéric Sirois¹, and Francesco Grilli²

¹*Polytechnique Montréal, Montréal, Canada*

²*Karlsruhe Institute of Technology, Karlsruhe, Germany*

Abstract

The H-formulation, used abundantly for the simulation of high temperature superconductors, has shown to be a very versatile and easily implementable way of modeling electromagnetic phenomena involving superconducting materials. However, the simulation of a full vector field in current-free domains unnecessarily adds degrees of freedom to the model, thereby increasing computation times. In this contribution, we implement the well known H- ϕ formulation in COMSOL Multiphysics in order to compare the numerical performance of the H and H- ϕ formulations in the context of computing the magnetization of bulk superconductors. We show that the H- ϕ formulation can reduce the number of degrees of freedom and computation times by nearly a factor of two for a given relative error. The accuracy of the magnetic fields obtained with both formulations are demonstrated to be similar. The computational benefits of the H- ϕ formulation are shown to far outweigh the added complexity of its implementation, especially in 3-D. Finally, we identify the ideal element orders for both H and H- ϕ formulations to be quartic in 2-D and cubic in 3-D, corresponding to the highest element orders implementable in COMSOL.

1 Introduction

The modeling of the electromagnetic behavior of superconducting materials is a crucial aspect in the development of new technologies involving high temperature superconductors (HTS). The simulation of magnetic fields produced by HTS is especially important to predict and investigate the possible applications of HTS without having to physically produce experiments, which require much more time and resources. Over the years, the Finite Element Method (FEM) has shown to be one of the most reliable computational methods to simulate electromagnetic fields of HTS, with many different formulations adopted depending on the application of interest.

In the superconductivity community, the H-formulation, which uses a combination of Faraday's and Ampere's laws to solve for the magnetic field,

has been widely used for the modeling of HTS. Its applications vary remarkably, including the magnetization [1–8], demagnetization [9–11] and magnetic levitation [12–15] of bulk superconductors, AC losses in superconducting windings [16–23], etc. More details on the possibilities offered by the H-formulation can be found in two recently published review articles [23, 24].

Brambilla et al. and J.P. Webb describe the many reasons for the appeal of this formulation [16, 25]. First, the use of edge elements allows the field to be discontinuous in the normal direction to the element edge, enabling the field to abruptly change direction near sharp corners. Additionally, the uniqueness of the solution for the magnetic field does not require any choice of gauge, as required by other formulations solving for the magnetic vector and/or

scalar potentials. Moreover, the boundary conditions are easily imposed in this formulation due to the intuitive nature of the magnetic field as a dependent variable. Finally, the resulting dependent variables do not need extra calculations in order to obtain the magnetic field, as opposed to other formulations, such as the \mathbf{A} - ϕ formulation, that must calculate spatial derivatives of \mathbf{A} to obtain \mathbf{H} . This last point is important because it reduces the numerical error when compared to other formulations, since computing the derivative introduces additional local inaccuracies in the simulated results. Note that the divergence-free condition of Maxwell's equations is not automatically enforced with curl elements, as previously assumed. The divergence-free condition is only met locally for elements of first order due to the discontinuities of the normal component of the field between elements [26]. However, in time-dependent simulations, the divergence-free condition is met at all times if the initial values are divergence-free [20].

Nevertheless, despite the renowned success of the H-formulation, this formulation still has its caveats. Namely, the solution of a vector field in the non-conducting regions, typically air, increases the size of the linear matrix to be solved. In reality, a full vector field is not required in current-free regions. Hence, although the H-formulation has been satisfactory for many applications, the computation times achieved using this formulation are longer than other formulations using nodal elements with the same mesh discretization [27]. Furthermore, the H-formulation requires a dummy resistivity in the air regions, which is non-physical and degrades the matrix conditioning. The main reason for implementing the H-formulation everywhere in space is because it is simple to do, which explains why it is being used by over 45 research groups in the applied superconductivity community in the COMSOL Multiphysics finite element program [24, 28].

On the other hand, mixed formulations such as the H- ϕ , T- ϕ and T- Ω are often used in electromagnetics dedicated FEM software [29–32]. However, many of these software have their own shortcomings when applied to superconductivity: the non-linear resistivity cannot always be implemented depending on the software used and when it is possible, the conver-

gence of the solution is not always favorable. Several researches have used the H- ϕ formulation to simulate superconductors in open-source software such as GetDP [33–35], which provides greater customizability than COMSOL, but with a steeper learning curve and less support than commercial software.

In this work, we implement the H- ϕ formulation in COMSOL Multiphysics 5.5 by coupling the magnetic field variables to the magnetic scalar potential through a custom-parameterized weak formulation. Surprisingly, such an implementation in COMSOL does not seem to have been reported yet, despite its possibility since the earliest versions of COMSOL. The simulations conducted in this work have been tested on COMSOL version 4.3b and work as well as in the newest version of COMSOL. With a simple simulation of a 2-D and 3-D HTS bulk magnetized in a uniform applied field, we compare the computation times and accuracies between the H and H- ϕ formulations.

2 H- ϕ formulation

2.1 Governing equations

The H- ϕ formulation combines the magnetic field, \mathbf{H} , and magnetic scalar potential, ϕ , in conducting and non-conducting regions, respectively. Based on figure 1, the H- ϕ formulation can be stated as follows: one solves for the full vector \mathbf{H} in the superconducting regions (Ω_c , where currents can exist), and only for the magnetic scalar potential ϕ in the air regions (Ω_{nc} , which are current-free). This allows for a reduction of the number of DOF in the problem. In this article, we refer to \mathbf{H} and \mathbf{h} as the magnetic fields in the H and ϕ formulations, respectively. We can then derive \mathbf{h} from ϕ as follows

$$\mathbf{h} = -\nabla\phi. \quad (1)$$

This definition forces \mathbf{J} to be zero in the non-conducting regions since $\mathbf{J} = \nabla \times \mathbf{h} = \nabla \times (-\nabla\phi) = 0$ (the curl of a gradient is identically zero).

To derive a useful equation from (1), one can use the divergence-free equation $\nabla \cdot \mathbf{B} = 0$, and assume

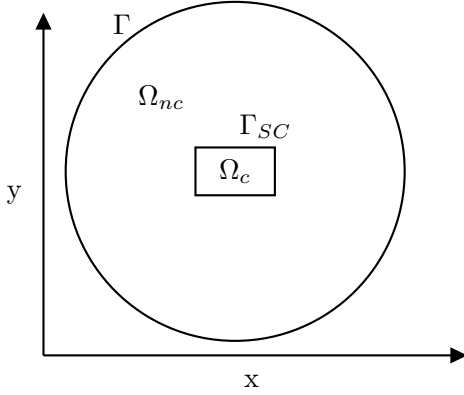


Figure 1: Simple domain investigated in this contribution, showing one conducting region Ω_c , one non-conducting region Ω_{nc} . We denote the boundary between these two domains as Γ_{SC} and the external boundary of the air domain as Γ .

that $\mathbf{B} = \mu_0 \mathbf{h}$ in the whole simulated space containing the air and superconducting domains. We then obtain $\nabla \cdot (\mu_0 \mathbf{h}) = \mu_0 \nabla \cdot (-\nabla \phi) = 0$, which can be rewritten as Laplace's equation, i.e.

$$\text{In } \Omega_{nc}: \quad \nabla \cdot \nabla \phi = 0. \quad (2)$$

In the conducting regions, the governing equation is the conventional H-formulation expression, given by:

$$\text{In } \Omega_c: \quad \nabla \times (\rho \nabla \times \mathbf{H}) = -\mu_0 \frac{d\mathbf{H}}{dt}, \quad (3)$$

where the resistivity ρ is nonlinear in the case of superconductors, therefore it cannot be taken out of the external curl operator. As mentioned earlier, when using the H-formulation in the whole simulation space, the resistivity of air must be set to a non-zero value in order to obtain better convergence. This problem does not exist when using the magnetic scalar potential in the air domains, since no resistivity must be specified.

In order to generate a background magnetic field, we use a Dirichlet boundary condition in terms of ϕ on Γ . For example, if we want to apply a field in the $+\hat{y}$ direction, the Dirichlet condition reads $\phi = -H_0(t)y$, with $H_0(t)$ being the time-dependent applied field.

Finally, we use curl edge elements in the conducting regions since we are solving for the vector \mathbf{H} . We use Lagrange nodal elements in the non-conducting regions to solve for the scalar ϕ . Knowing the properties of the elements used is important when coupling the two formulations, as described in the next section. In the case of curl elements, the tangential component of the dependent variable is constant along the element edges. On the other hand, Lagrange elements are nodal, meaning that the dependent variables are free to vary along the element edges.

2.2 Coupling relations

We first begin by coupling ϕ to the \mathbf{H} variables. Since we have edge elements in the conducting domain, the DOF are given by the tangential component of the dependent variables on the element edges. Thus, we constrain the tangential component of \mathbf{H} to be equal to the tangential component of \mathbf{h} with the use of a constraint enforced in the strong form (called pointwise constraint in the Comsol language). This can be written as:

$$\hat{\mathbf{n}} \times \mathbf{H} = \hat{\mathbf{n}} \times \mathbf{h}, \quad (4)$$

where $\hat{\mathbf{n}}$ is the unit normal vector to Γ_{SC} .

Coupling the \mathbf{H} variables to ϕ is slightly more challenging. We first write (2) in its weak form, which is easily shown to be:

$$\int_{\Omega_{nc}} \nabla \phi \cdot \nabla v \, dV - \int_{\Gamma_{SC}} \hat{\mathbf{n}} \cdot \nabla \phi \, v \, dA = 0, \quad (5)$$

where v is a test function and $\hat{\mathbf{n}}$ is the vector normal to the Γ_{SC} boundary. In this equation, the first term generates Gauss' law ($\nabla \cdot \nabla \phi = 0$), while the second term allows fixing the normal flux of \mathbf{h} ($= -\nabla \phi$) on the Γ_{SC} boundary.

Since we have already constrained the tangential component of \mathbf{H} , we must now couple the normal components in the weak formulation in order to completely define the physics at the interface between the \mathbf{H} and ϕ domains. This is done by inserting \mathbf{H} in the second term of (5), so that the equation becomes:

$$\int_{\Omega_{nc}} \nabla \phi \cdot \nabla v \, dV - \int_{\Gamma_{SC}} \hat{\mathbf{n}} \cdot (\nabla \phi + \mathbf{H}) \, v \, dA = 0, \quad (6)$$

therefore setting the normal component of \mathbf{h} equal to the normal component of \mathbf{H} .

Instructions for modeling the equations of this section in COMSOL Multiphysics are detailed in the Appendix.

3 Magnetization simulations

We evaluate the computational efficiency of the $H\text{-}\phi$ formulation with a simple simulation of a bulk HTS magnetized by zero field cooling (ZFC) in a uniform background field of 5 T. The magnetic field is slowly ramped up and is brought back down using a smoothed triangular function of one second in duration. We use COMSOL Multiphysics 5.5 to solve the above equations with the finite element method. The personal computer used to perform the simulations in this paper has an Intel(R) Core(TM) i7-3770 processor with 32 Gb of random access memory.

The HTS material considered is a $\text{YBa}_2\text{Cu}_3\text{O}_{7-x}$ cylindrical bulk of 1 cm radius and 1 cm height. The non-linear resistivity of the HTS is modeled using the power law model [36]:

$$\rho = \frac{E_c}{J_c(\|\mathbf{B}\|)} \left(\frac{\|\mathbf{J}\|}{J_c(\|\mathbf{B}\|)} \right)^{n-1}, \quad (7)$$

with \mathbf{J} being the current density, $J_c(\|\mathbf{B}\|)$ being the field dependent critical current density, $n = 25$, and $E_c = 1 \mu\text{V}/\text{cm}$. We use Superconducting QUantum Interference Device (SQUID) measurements obtained by Can Superconductors [37] as an input for modeling the field dependence of the critical current density at 77 K, as shown in figure 2. The SQUID data is smoothed in order to obtain better convergence. We compare the results obtained from the $H\text{-}\phi$ formulation to those obtained from the H -formulation in both 2-D Cartesian and 3-D simulations.

We use a MULTifrontal Massively Parallel sparse direct Solver (MUMPS) for the H -formulation and a PARallel Sparse Direct Solver (PARDISO) for the $H\text{-}\phi$ formulation, since these solvers were found to give better computation times and accuracies for the respective formulations both in 2-D and 3-D.

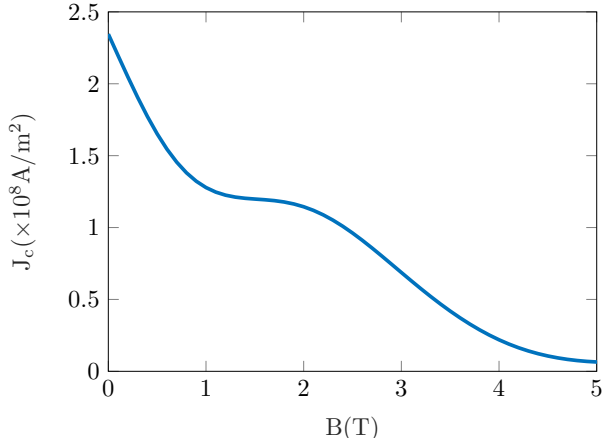


Figure 2: Smoothed function of the $J_c(\|\mathbf{B}\|)$ data measured by Can Superconductors [37].

3.1 2-Dimensional analysis

The geometry used to simulate the HTS bulk in 2-D in Cartesian form is shown in figure 1, with the air domain having a radius of 15 cm and the rectangular region being a cross section of the 2×1 cm HTS domain. We use a triangular mesh on the whole domain of simulation, with a mesh 5 times finer inside the superconducting domain than in the air domain.

The norm of the magnetic field after the ZFC process is shown in figure 3a), where the result was calculated using 2594 quartic elements with the H -formulation. This solution constitutes our reference solution. We compare this result with the one obtained with 2594 quartic elements in the $H\text{-}\phi$ formulation. For this, we compute the relative error (in percent) between both results using

$$e = \left| \frac{\|\mathbf{H}\| - \|\mathbf{H}_{\text{ref}}\|}{\|\mathbf{H}_{\text{ref}}\|} \right| \times 100\%, \quad (8)$$

where $\|\mathbf{H}_{\text{ref}}\|$ is the norm of \mathbf{H} in the reference solution obtained with the H -formulation. Throughout this work, we use the same order of curl and Lagrange elements for the $H\text{-}\phi$ formulation. We use COMSOL's *Join* feature to calculate the error between different simulation results.

The percent error between formulations is shown

in figure 3b). Notice that the regions of maximal error occur where the \mathbf{H} -field varies more drastically at the edges of the bulk, more specifically at the corners and along the center of the top and bottom edges. This induced error most likely comes from the connection of the normal \mathbf{B} components across elements with curl and Lagrange shape functions. However, even at these points, the maximum error is below 0.3 % when using 2594 quartic elements. This error increases when fewer and lower order elements are used. At distances far from the bulk, the fields are practically equivalent, with a percent error less than 0.01%.

Finally, the worst error is found in the superconducting domain to be ~ 0.41 %, most likely emerging from the fact that the norm of the field is nearly zero at these points, therefore blowing up the denominator in (8).

3.1.1 2-D H-formulation

In order to properly compare our simulation results, we must determine an accurate representation of the magnetic field produced by the HTS. We begin by simulating the well documented H-formulation and use the standard FEM method of varying the number of DOF in the model to verify the convergence of the results. We calculate the average of the norm of the magnetic field inside the superconducting region after the ZFC process as our observable quantity to accomplish the convergence rate analysis. In the rest of the paper, we shall refer to this observable quantity as the “convergence parameter”. With increasingly finer mesh and element order, the solution is said to be converged when increasing the number of DOF does not significantly affect the convergence parameter value.

Figure 4a) summarizes the convergence rates of the average field with linear, quadratic and quartic elements using the H-formulation. According to the figure, quadratic elements with at least $\sim 13,000$ DOF and quartic elements with at least $\sim 9,000$ DOF are needed for a convergent result of ~ 443 kA/m. On the other hand, the solution barely converges even with the highest number of DOF for linear elements.

By referring to figure 4a), we use 2594 quartic el-

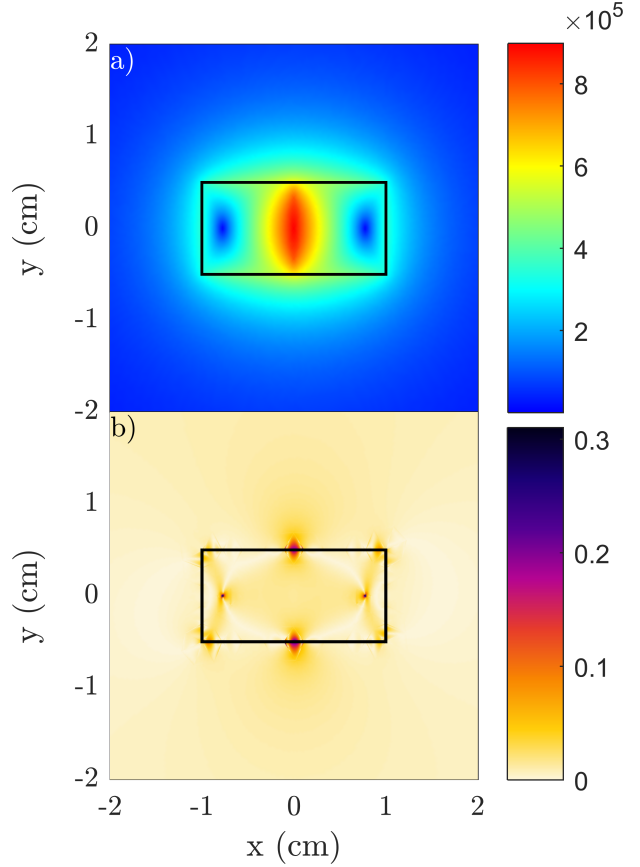


Figure 3: a) Norm of the magnetic field, $\|\mathbf{H}\|$ (A/m), calculated using the H-formulation with 2594 quartic elements after the background field is ramped down to zero. This result is taken as the reference for comparison with other simulations, as explained in the text. b) Percent error of the magnetic field calculated at each point using the H- ϕ formulation, with the H-formulation as reference, both using 2594 quartic elements. The maximum value of the colorbar has been reduced from 0.41 % to 0.3 % for clarity. The values corresponding to 0.41 % are the two points inside the superconducting domain where the field is nearly zero. The error of the field near the edges of the bulk still remains below 0.3 %.

ements with 47,000 DOF as our “exact” solution, shown in figure 3a). This solution will be used as

a reference in order to compare with other simulation results. The magnetic field calculated in this simulation will be referred to as \mathbf{H}_{ref} in the rest of this section.

Figure 4b) illustrates the percent error calculated using different element orders and mesh discretizations for the H-formulation. The error is calculated by integrating (8) over the superconducting domain and dividing by the area, while using \mathbf{H}_{ref} as reference. The behavior is very similar to the convergence rates of figure 4a). The percent error for linear elements remains above 1.7 % even for the highest number of DOF, while the error for quadratic and quartic elements is negligible once the convergence of the norm of \mathbf{H} is achieved. Note that quartic elements are slightly more accurate than quadratic elements for a given number of DOF.

Finally, the computation times of each simulation in figure 4a) are shown in figure 4c). In addition to the poor results obtained with linear curl elements, the computation times are even higher than quadratic and quartic elements for a given number of DOF. This conclusion seems surprising since most authors use first order edge elements with the H-formulation, which helps to achieve good convergence in AC loss computations at power frequencies [38]. However, the slow magnetization process simulated in this paper has not shown any convergence problem related to the order of the basis functions, which opens the door to further exploration. Nevertheless, in the scope of this paper, we can clearly state that quartic elements are favorable in 2-D, both for their computation times as well as their accuracy. Note that quartic elements are the highest element order available for curl elements in COMSOL in 2-D.

3.1.2 2-D H- ϕ formulation

We follow the procedure of the last section to determine the ideal element order of the H- ϕ formulation and compare the results with the H-formulation.

The convergence parameter as a function of DOF shows similar behavior as the one calculated in the H-formulation of figure 4a), as seen in figure 4d). However, for the H- ϕ formulation, the quadratic elements converge slightly more quickly than quartic elements.

Additionally, linear elements seem to converge above $\sim 22,700$ DOF.

We determine the accuracy of the H- ϕ formulation by calculating the percent error with \mathbf{H}_{ref} as reference, represented in figure 4e). We find that linear elements still do not accurately represent the exact solution, while quadratic and quartic elements have negligible error ($< 0.45\%$) for more than $\sim 12,000$ DOF. Comparing with the H-formulation errors of figure 4b), the use of linear elements seems more forgiving in the H- ϕ formulation, since the error is systematically smaller in this case. Nevertheless, we still find that quartic elements are slightly more accurate than quadratic elements, although the difference is negligible.

Lastly, the computation times for the different element orders are compared in figure 4f). We find that the computation times are similar for fewer DOF, while these times are significantly higher for quartic elements at higher DOF. We find that quadratic elements yield less computation times than linear and quartic elements for the same number of DOF.

Comparing figures 4a), b) and c) with figures 4d) e) and f), we find the main advantage of using the H- ϕ formulation. In the case of the H- ϕ simulations, the error becomes negligible for nearly half the amount of DOF than that of the H-formulation for quadratic and quartic elements. Furthermore, the computation times are nearly three times faster for the H- ϕ formulation for the most accurate solution obtained, representing a percent error of only 0.015 %. The computation time difference is not as drastic for lower amounts of DOF, but the H- ϕ formulation is still significantly faster.

For a final comparison, we consider the computational time required for each formulation and element order to obtain a relative error of 0.5%, as shown in table 1. We find that quartic elements need the lowest amount of time to reach an error of 0.5% in both formulations. While the improvement in computation time for the H- ϕ formulation is not substantial (35 seconds), the improvement will certainly increase for more complex models requiring more degrees of freedom.

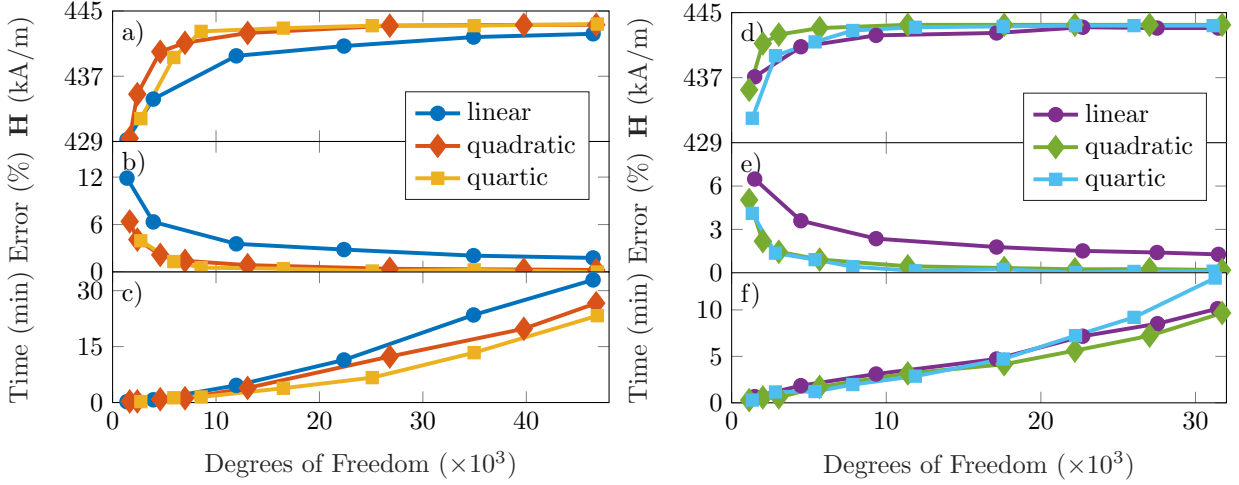


Figure 4: Comparison between 2-D simulations of the H and H- ϕ formulations with linear, quadratic and quartic elements. a) and d) show the convergence rate of the average field over the superconducting domain as a function of DOF in the H and H- ϕ formulations, respectively. b) and e) show the percent error relative to 2594 quartic curl elements simulated in the H-formulation as a function of DOF in the H and H- ϕ formulations, respectively. Finally, computation times of the H (c) and H- ϕ (f) formulations as a function of DOF are shown. A MUMPS direct solver is used for the H-formulation, while a PARDISO solver is used for the H- ϕ formulation.

Table 1: Computation times of the H and H- ϕ formulations in 2-D in order to achieve a relative error of 0.5%

Order	H time (min)	H- ϕ time (min)
1	>45	>10
2	10.62	3.01
4	2.42	1.84

3.2 3-D analysis

The three-dimensional analysis is carried out by following the same procedure as in the 2-D case. This time, we use the complete cylindrical bulk of 1 cm radius and 1 cm height, with an air domain in the form of a sphere of 15 cm radius. As in the 2-D case, the physics coupling of the H- ϕ formulation is done by using equations (4) and (6). We apply the magnetic field along the z-axis, corresponding to the axial direction of the cylinder.

3.2.1 3-D H-formulation

In order to obtain an accurate solution, we investigate the convergence of the solutions by varying the mesh discretization and element order with the H-formulation. The convergence parameter is obtained by calculating the average field over the superconducting domain. In the 3-D case, the highest available order of elements in COMSOL is cubic, so we compare the convergence rates of linear, quadratic and cubic elements, illustrated in figure 5a).

Notice that cubic elements converge slightly faster than quadratic elements, yet both element orders converge to the same value of ~ 403 kA/m. Conversely, linear elements converge more slowly and to a value slightly higher than quadratic and cubic elements at ~ 406 kA/m.

We determine the percent error of each simulation with respect to the number of DOF using the solution with 157,400 DOF and 8325 cubic elements as reference. We take this solution as a reference, not only

because it is more than converged in figure 5a), but it is also visually smoother than other converged results. Accordingly, we calculate the average percent error over the superconducting domain by integrating (8) for the different element orders, as summarized in figure 5b).

Similarly to the 2-D case, we find that linear elements are not well suited for an accurate solution in 3-D. Even for the highest number of DOF of 160,000, the percent error is still 16 %. Quadratic elements are more accurate, with the lowest error being 3 %. Ultimately, cubic elements show the most accurate results even for numbers of DOF as low as 43,800. Thus, cubic elements should be used in the 3-D H-formulation if the most accurate solution is desired.

However, despite the accuracy of cubic elements, their computation time is significantly longer than that of lower order elements, as demonstrated in figure 5c). For the highest amount of DOF simulated, cubic elements take approximately twice the amount of time required for quadratic elements and about four times longer than linear elements for the same number of DOF. Therefore, there is a compromise between accuracy and computation time for quadratic and cubic elements. Although there is not a large discrepancy between their accuracies, the computation time of quadratic elements is drastically faster than cubic elements for a given number of DOF.

3.2.2 3-D H- ϕ formulation

We analyze the three dimensional H- ϕ formulation by first performing a convergence rate analysis with the norm of \mathbf{H} as the parameter. As shown in figure 5d), the cubic elements converge very rapidly to ~ 403 kA/m, the same value as the H-formulation result. On the other hand, quadratic element results converge slower, with a convergence value slightly lower at ~ 401 kA/m. This is surprising, considering that quadratic and quartic elements converged to approximately the same value in 2-D, while the same can be said with quadratic and cubic elements in the 3-D H-formulation. Nevertheless, the difference between converged values is still less than 1 %. Finally, linear elements converge at nearly the same rate as quadratic elements, but with a higher convergence

value of ~ 408 kA/m.

We proceed to calculate the percent error between the H and H- ϕ formulation results simulated with 157,400 DOF and 8325 cubic elements, as illustrated in figure 5e). We find that the percent error remains relatively low ($<1.5\%$) for cubic elements above 27,000 DOF. Using quadratic elements yields error values above 2.5% for the highest number of DOF simulated, with the error remaining marginally higher than cubic elements for a given number of DOF. Linear elements still present poor results, with the lowest error remaining at 10.2 % for 56,500 DOF. Accordingly, the results are very similar to the H-formulation case: cubic elements are ideal for the most accurate solutions, with quadratic elements still providing relatively accurate results.

We compare the computation times between different element orders in figure 5f). Notice that linear and quadratic elements have very similar computational efficiencies for a given DOF, while cubic elements yield much higher computation times.

Finally, we compare the computation times required to obtain a relative error of 3% as a function of element order and model formulation. As shown in table 2, the time required to obtain a relative error of 3% is nearly halved in the H- ϕ formulation when compared to the result obtained with the H-formulation using cubic elements. The computation times are nearly three times faster in the H-formulation and 0.63 times faster in the H- ϕ formulation for cubic elements than for quadratic elements, so we conclude that cubic elements are ideal in both formulations in 3-D. Finally, the H- ϕ formulation is nearly twice as fast as the H-formulation when considering cubic elements.

Table 2: Computation times of the H and H- ϕ formulations in 3-D in order to achieve a relative error of 3%

Order	H time (hrs)	H- ϕ time (hrs)
1	>2.3	>1.2
2	3.20	1.00
3	1.15	0.63

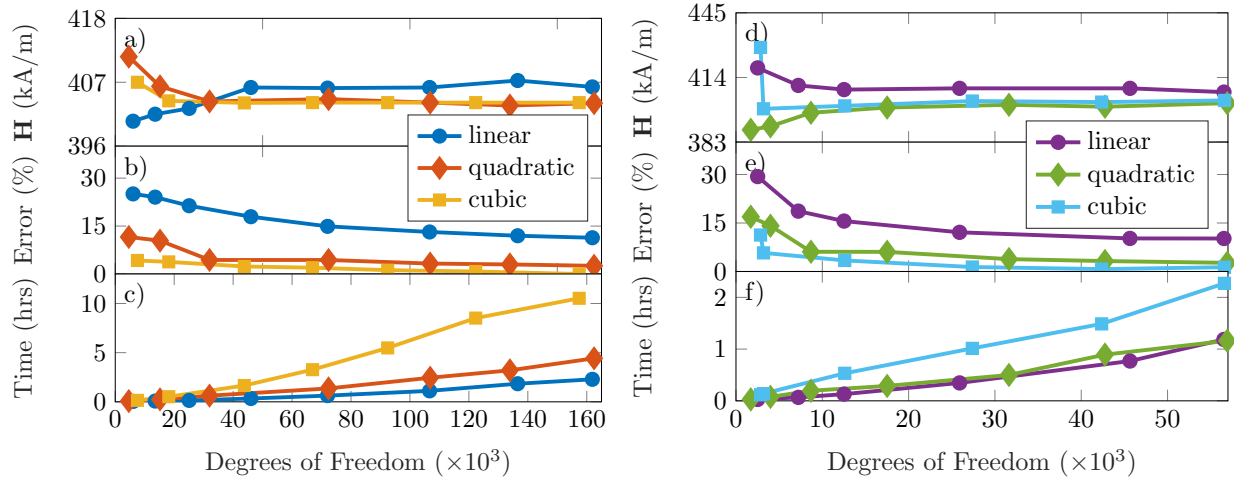


Figure 5: Comparison between 3-D simulations of the H and H- ϕ formulations with linear, quadratic and cubic elements. a) and d) show the convergence rates of the average field over the superconducting domain as a function of DOF in the H and H- ϕ formulations, respectively. b) and e) show the percent error relative to 8325 cubic curl elements simulated in the H-formulation as a function of DOF in the H and H- ϕ formulations, respectively. Finally, computation times of the H (c) and H- ϕ (f) formulations as a function of DOF are shown. A MUMPS direct solver is used for the H-formulation, while a PARDISO solver is used for the H- ϕ formulation.

4 Conclusion

In this work, we implemented the H- ϕ formulation in COMSOL Multiphysics in order to compare its performances with the well-documented H-formulation in the context of the magnetization of bulk superconductors. Using standard ZFC magnetization simulations in 2-D and 3-D, we studied the accuracy and computation times obtained from the different formulations with varied element orders and mesh discretizations.

By comparing simulation results of 2594 quartic elements in the H and H- ϕ formulations in 2-D, we found that the percent error between formulations remains below 0.3 % at the edges of the superconducting domain, where the field varies more drastically. The percent error is below 0.01 % for fields far from the bulk, showing that the formulations give nearly equivalent results even though different element types were used.

We identified the ideal element order to be the

highest order implementable in COMSOL Multiphysics, regardless of formulation or dimension. Accordingly, the ideal element order is quartic in 2-D and cubic in 3-D for both formulations. The choice of element orders is clear in 2-D: both the accuracies and computation times are improved for quartic elements. In order to obtain a relative error of 0.5%, the computation times were found to be more than 1.5 times quicker using quartic elements than quadratic elements. In 3-D, cubic elements provide greater accuracy than quadratic elements for a given number of DOF, but their computation times are much higher with their accuracy being merely slightly better. Nevertheless, we find that cubic elements used in the H- ϕ formulation still solve virtually twice as fast as cubic elements in the H-formulation when comparing the computation times required for an error of 3%.

Further work should be conducted in order to determine if mixing Lagrange and curl element orders in the H- ϕ formulation yields better results than using

the same order for both types of elements. In addition, more complete simulations could be realized in order to generalize the observations presented in this work.

5 Acknowledgements

The authors would like to acknowledge Bruno Alves for interesting discussions concerning the finite element method and Can Superconductors for providing the field dependent critical current density data.

This work was supported by the Fonds de recherche du Québec — Nature et Technologies (FRQNT) and TransMedTech Institute and its main funding partner, the Canada First Research Excellence Fund.

6 Appendix: COMSOL implementation of the \mathbf{H} - ϕ formulation

In this Appendix, we describe the implementation of the \mathbf{H} - ϕ formulation in COMSOL. The model used in this work will be available on the HTS modelling website [39].

Similarly to the \mathbf{H} -formulation, there are two equivalent ways of implementing the \mathbf{H} - ϕ formulation: by defining our own PDEs or using the predefined COMSOL *Magnetic Field Formulation* (MFH) and *Magnetic Field No Currents* (MFNC) modules. We describe the more general 3-D implementation, the 2-D case easily follows.

6.1 PDE implementation

The PDE implementation follows from the equations laid out in Sec. 2. The \mathbf{H} physics is implemented using the *General Form PDE* physics to introduce (3) in the superconducting domain, as done in the regular \mathbf{H} -formulation. We introduce the ϕ physics in the non-conducting domain with a *Weak Form PDE* node and implement the first term of (5), corresponding to the Lagrange equation. In COMSOL notation,

this is given in 3-D by:

$$-u_x * \text{test}(u_x) - u_y * \text{test}(u_y) - u_z * \text{test}(u_z), \quad (9)$$

where u is the dependent variable of the ϕ physics, u_i is the derivative of u with respect to i , and $\text{test}(u)$ is the test function defined by COMSOL. By defining this expression in the *Weak Form PDE* node, COMSOL automatically takes the integral of the expression over the selected domain and sets it equal to zero. Note that the Laplace equation can also be implemented using the *Coefficient Form PDE* module.

Finally, we apply the background field by using a regular *Dirichlet Boundary Condition* node, keeping in mind that the negative of the gradient of the inserted expression generates the applied background magnetic field.

In order to couple the physics together, we use the procedure outlined in Sec. 2.2. First, the tangential components of the \mathbf{H} -field are constrained to the tangential components of the \mathbf{h} -field by using a *Constraint* node in the \mathbf{H} physics with the expressions

$$\begin{aligned} tH_x + uT_x &= 0 \\ tH_y + uT_y &= 0 \\ tH_z + uT_z &= 0 \end{aligned}$$

introduced in the three boxes supplied. Here, tH_i represents the tangential component of the \mathbf{H} -field in the i -direction and uT_i represents the tangential derivative of u in the i direction. The constraint settings must be set to *Current physics (internally symmetric)* in order to get a unidirectional constraint and not overconstrain the \mathbf{h} -field.

Equating the normal components of the magnetic fields can easily be done with the *Flux/Source* node in the ϕ physics. The equation defined under this node is given by $-\mathbf{n} \cdot \nabla u = g$, where g is the boundary source term. We therefore set $g = n_x * H_x + n_y * H_y + n_z * H_z$, keeping in mind that the \mathbf{h} -field is given by $-\nabla u$, so that g should be positive. Here, n_x , n_y , and n_z are the components of the vector normal to the surface. We should also pay careful attention to the normal vectors used, since the normal of one domain is equal to the negative of the normal of the other. In this case, simply typing n_x , n_y and

n_z supplies the normal vector on Γ_{SC} of the air domain, since we applied the *Flux/Source* node in the ϕ physics.

6.2 MFH + MFNC implementation

The H - ϕ formulation can effortlessly be implemented with built-in MFH and MFNC modules. Although less control is given on defined variables in this case, the predefined physics modules make it very easy to carry out simulations without the trouble of defining all necessary variables. However, for reasons unknown to the authors, quartic elements are unavailable in the 2-D MFH module.

Let's start with the \mathbf{H} physics, imposed using the MFH module. The superconducting physics is simply imposed by using a nonlinear resistivity in the *Faraday's Law* node. We then couple to the MFNC physics by using a *Magnetic Field* node, which generates a magnetic field at the boundary of the superconductor. The input is simply (mfnc.Hx,mfnc.Hy,mfnc.Hz), where mfnc.H is the magnetic field calculated in the MFNC module. COMSOL automatically equates the tangential components in this formulation (as can be seen in the *equation view*), since we are using edge elements. Again, we set the constraint settings to *Current physics (internally symmetric)* in order to get a unidirectional constraint.

Finally, the ϕ physics is implemented using the MFNC module. There are two ways of applying the background field, either by applying it at the boundary using a *Magnetic Flux Density* node, or by solving for the reduced field in the MFNC node and imposing a background field. In the latter case, an *External Magnetic Flux Density* node needs to be applied at the domain boundary in order to generate the field. However, no significant difference has been observed between the two methods of imposing the background field. The coupling between the MFNC and MFH physics is done with a *Magnetic Flux Density* node with (mfh.Bx, mfh.By, mfh.Bz) as input on Γ_{SC} , where mfh.B is the magnetic flux density calculated using the MFH physics.

References

- [1] Z. Hong, A. M. Campbell, and T. A. Coombs. Numerical solution of critical state in superconductivity by finite element software. *Supercond. Sci. Technol.*, 19(12):1246–1252, 2006.
- [2] M. D. Ainslie, H. Fujishiro, T. Ujiie, J. Zou, A. R. Dennis, Y. H. Shi, and D. A. Cardwell. Modelling and comparison of trapped fields in (RE)BCO bulk superconductors for activation using pulsed field magnetization. *Supercond. Sci. Technol.*, 27(6):9, 2014.
- [3] M. D. Ainslie and H. Fujishiro. Modelling of bulk superconductor magnetization. *Supercond. Sci. Technol.*, 28(5):53002, 2015.
- [4] M. P. Philippe, M. D. Ainslie, L. Wéra, J. F. Fagnard, A. R. Dennis, Y. H. Shi, D. A. Cardwell, B. Vanderheyden, and P. Vanderbemden. Influence of soft ferromagnetic sections on the magnetic flux density profile of a large grain, bulk Y-Ba-Cu-O superconductor. *Supercond. Sci. Technol.*, 28(9), 2015.
- [5] J. Zou, M. D. Ainslie, H. Fujishiro, A. G. Bhagurkar, T. Naito, N. Hari Babu, J. F. Fagnard, P. Vanderbemden, and A. Yamamoto. Numerical modelling and comparison of MgB₂ bulks fabricated by HIP and infiltration growth. *Supercond. Sci. Technol.*, 28(7), 2015.
- [6] S. Zou, V. M. R. Zermeno, and F. Grilli. Influence of Parameters on the Simulation of HTS Bulks Magnetized by Pulsed Field Magnetization. *IEEE Trans. Appl. Supercond.*, 26(4):1–5, June 2016.
- [7] M. Kapolka, V. M. R. Zermeno, S. Zou, A. Morandi, P. L. Ribani, E. Pardo, and F. Grilli. Three-Dimensional Modeling of the Magnetization of Superconducting Rectangular-Based Bulks and Tape Stacks. *IEEE Trans. Appl. Supercond.*, 28(4):1–6, June 2018.

- [8] Kai Yuan Huang, Yunhua Shi, Jan Srpčič, Mark D Ainslie, Devendra K Namburi, Anthony R Dennis, Difan Zhou, Martin Boll, Mykhaylo Filipenko, Jan Jaroszynski, Eric E Hellstrom, David A Cardwell, and John H Durrell. Composite stacks for reliable > 17 T trapped fields in bulk superconductor magnets. *Supercond. Sci. Technol.*, 33(2):02LT01, January 2020.
- [9] S Celebi, F Sirois, and C Lacroix. Collapse of the magnetization by the application of crossed magnetic fields: Observations in a commercial Bi:2223/Ag tape and comparison with numerical computations. *Supercond. Sci. Technol.*, 28(2):025012, February 2015.
- [10] M. Kapolka, J. Srpčic, D. Zhou, M. D. Ainslie, E. Pardo, and A. R. Dennis. Demagnetization of Cubic Gd-Ba-Cu-O Bulk Superconductor by Crossed-Fields: Measurements and Three-Dimensional Modeling. *IEEE Trans. Appl. Supercond.*, 28(4):1–5, June 2018.
- [11] Mehdi Baghdadi, Harold S. Ruiz, and Timothy A. Coombs. Nature of the low magnetization decay on stacks of second generation superconducting tapes under crossed and rotating magnetic field experiments. *Sci. Rep.*, 8(1):1342, January 2018.
- [12] F. Sass, G. G. Sotelo, R. De Andrade, and Frédéric Sirois. H-formulation for simulating levitation forces acting on HTS bulks and stacks of 2G coated conductors. *Supercond. Sci. Technol.*, 28(12), 2015.
- [13] Francesco Grilli, Antonio Morandi, Federica De Silvestri, and Roberto Brambilla. Dynamic modeling of levitation of a superconducting bulk by coupled H-magnetic field and Arbitrary Lagrangian-Eulerian formulations. *Supercond. Sci. Technol.*, 31(12), 2018.
- [14] Loïc Quéval, Kun Liu, Wenjiao Yang, Víctor M R Zermeno, and Guangtong Ma. Superconducting magnetic bearings simulation using an H -formulation finite element model. *Supercond. Sci. Technol.*, 31(8):084001, August 2018.
- [15] F. Ferreira da Silva and P. J. Costa Branco. Study of a cylindrical geometry design for a zero field cooled Maglev system. *Supercond. Sci. Technol.*, 32(6):065004, May 2019.
- [16] Roberto Brambilla, Francesco Grilli, and Luciano Martini. Development of an edge-element model for AC loss computation of high-temperature superconductors. *Supercond. Sci. Technol.*, 20(4), 2007.
- [17] D. N. Nguyen, J. Y. Coulter, J. O. Willis, S. P. Ashworth, H. P. Kraemer, W. Schmidt, B. Carter, and A. Otto. AC loss and critical current characterization of a noninductive coil of two-in-hand RABiTS YBCO tape for fault current limiter applications. *Supercond. Sci. Technol.*, 24(3):035017, January 2011.
- [18] Min Zhang, Jae-Ho Kim, Sastry Pamidi, Michal Chudy, Weijia Yuan, and T. A. Coombs. Study of second generation, high-temperature superconducting coils: Determination of critical current. *Journal of Applied Physics*, 111(8):083902, April 2012.
- [19] Mark D. Ainslie, Tim J. Flack, and Archie M. Campbell. Calculating transport AC losses in stacks of high temperature superconductor coated conductors with magnetic substrates using FEM. *Physica C: Superconductivity*, 472(1):50–56, January 2012.
- [20] Victor M. R. Zermeno, Francesco Grilli, and Frederic Sirois. A full 3D time-dependent electromagnetic model for Roebel cables. *Supercond. Sci. Technol.*, 26(5):052001, March 2013.
- [21] Jing Xia, Huadong Yong, and Youhe Zhou. Numerical simulations of the alternating current loss in round high-temperature superconducting wire with a hole defect. *Journal of Applied Physics*, 114(9):093905, September 2013.

- [22] Junjie Zhao, Yingxu Li, and Yuanwen Gao. 3D simulation of AC loss in a twisted multi-filamentary superconducting wire. *Cryogenics*, 84:60–68, June 2017.
- [23] Boyang Shen, Francesco Grilli, and Tim Coombs. Review of the AC loss computation for HTS using H formulation. *Supercond. Sci. Technol.*, 33(3):033002, March 2020.
- [24] Boyang Shen, Francesco Grilli, and Tim Coombs. Overview of H-Formulation: A Versatile Tool for Modeling Electromagnetics in High-Temperature Superconductor Applications. *IEEE Access*, 8:100403–100414, 2020.
- [25] J. B. Webb. Edge Elements and what they can do for you. *IEEE Trans. Magn.*, 1993.
- [26] Andy Tak Shik Wan. *Adaptive Space-Time Finite Element Method In High Temperature Superconductivity*. PhD thesis, Université de Montréal, July 2014.
- [27] Valtteri Lahtinen, Antti Stenvall, Frédéric Sirois, and Matti Pellikka. A Finite Element Simulation Tool for Predicting Hysteresis Losses in Superconductors Using an H-Oriented Formulation with Cohomology Basis Functions. *J Supercond Nov Magn*, 28(8):2345–2354, August 2015.
- [28] COMSOL: Multiphysics Software for Optimizing Designs. <https://www.comsol.com/>.
- [29] C.J. Carpenter. Comparison of alternative formulations of 3-dimensional magnetic-field and eddy-current problems at power frequencies. *Proc. Inst. Electr. Eng. UK*, 124(11):1026, 1977.
- [30] O. Biro, K. Preis, and K.R. Richter. Various FEM formulations for the calculation of transient 3D eddy currents in nonlinear media. *IEEE Trans. Magn.*, 31(3):1307–1312, 1995.
- [31] P. Zhou, Z. Badics, D. Lin, and Z.J. Cendes. Nonlinear T- Ω formulation including motion for multiply connected 3-d problems. *IEEE Trans. Magn.*, 44(6):718–721, 2008.
- [32] Opera — SIMULIA by Dassault Systèmes®. <https://www.3ds.com/products-services/simulia/products/opera/>.
- [33] Patrick Dular and Christophe Geuzaine. {GetDP} reference manual: The documentation for {GetDP}, a general environment for the treatment of discrete problems. <http://getdp.info/>, December 2019.
- [34] Loïc Burger, Christophe Geuzaine, Francois Henrotte, and Benoît Vanderheyden. Modelling the penetration of magnetic flux in thin superconducting films with shell transformations. *COMPEL*, 38(5):1441–1452, September 2019.
- [35] L Burger, I S Veshchunov, T Tamegai, A V Silhanek, S Nagasawa, M Hidaka, and B Vanderheyden. Numerical investigation of critical states in superposed superconducting films. *Supercond. Sci. Technol.*, 32(12):125010, December 2019.
- [36] Jakob Rhyner. Magnetic properties and AC-losses of superconductors with power law current-voltage characteristics. *Phys. C Supercond. Its Appl.*, 212(3-4):292–300, 1993.
- [37] Can Superconductors. <https://www.can-superconductors.com/levitation-bulk.html>.
- [38] Frédéric Sirois and Francesco Grilli. Numerical Considerations About Using Finite-Element Methods to Compute AC Losses in HTS. *IEEE Trans. Appl. Supercond.*, 18(3), 2008.
- [39] HTS modeling workgroup. <http://www.htsmodelling.com/>.